SOLAR RADIO BURSTS AT LOW FREQUENCIES

J. FAINBERG
Goddard Space Flight Center, Greenbelt, Md. 20771, U.S.A

Abstract. Properties of solar radio bursts observed by spacecraft at frequencies below several MHz are reviewed. In this frequency range most of the observed bursts are type III events (associated with particles) but several cases of type II emission (associated with shocks) have been reported. The analyses which lead to emission levels of type III solar bursts out to beyond 1 AU from the Sun also indicate that the low frequency radiation is observed at the harmonic of the emission region plasma frequency. Simultaneous particle and radio measurements imply that the bursts are generated near the leading edge of impulsive streams of solar electrons with energies extending from several hundred keV to several keV. Recent experiments measuring the direction of arrival of the radio emission allow the exciter particles to be tracked along the interplanetary magnetic field from regions near the Sun out to 1 AU.

1. Introduction

Satellite measurements of traveling solar radio bursts extend the range of observations of the origin of these phenomena from 5 $R_\odot$ on out to past 1 AU. In these regions the coronal properties change from the rigid rotation conditions near the solar surface and take on the flow characteristics of the solar wind.

Type III solar radio bursts generated by energetic particles moving outward along open magnetic field lines provide a very important and unique source of information about physical conditions along the path of the exciter particles. In many cases these radio measurements provide an important link between observations of phenomena occurring near the solar surface with extensive *in situ* observations of solar wind, energetic particles, and magnetic fields at 1 AU.

In this paper I will review some of the general properties of type III bursts in the two-decade frequency range extending from several MHz down to 30 kHz. A principal problem in this observational range has been the determination of an average emission level scale in order to relate the physical information derived from the radio bursts to specific coronal distances. I will discuss the radio studies relating to this and will then illustrate how, with such an emission level scale and with measurements of radio arrival directions, it has been possible to track the motion of the exciter particles along the interplanetary magnetic field out to 1 AU.

2. Properties of Type III Bursts

Type III bursts generally occur in groups of overlapping bursts. At low frequencies, where the radiation lasts for some tens of minutes, single bursts are not common except during quiet times. Although isolated single bursts occur rarely, it is generally assumed that complex events can be described as combinations of individual bursts. However, it may be that in such complex events other phenomena such as type II or type IV radiation are involved.

Gordon Newkirk, Jr. (ed.), Coronal Disturbances, 183–200.

Figure 1 shows a simple type III burst observed on the RAE-1 spacecraft (Weber *et al.*, 1971). The lower figure shows intensity-time profiles at 6 frequencies. The upper part shows the same burst observed by a multichannel receiver displayed in a frequency-time contour plot of 1 dB intensity intervals.

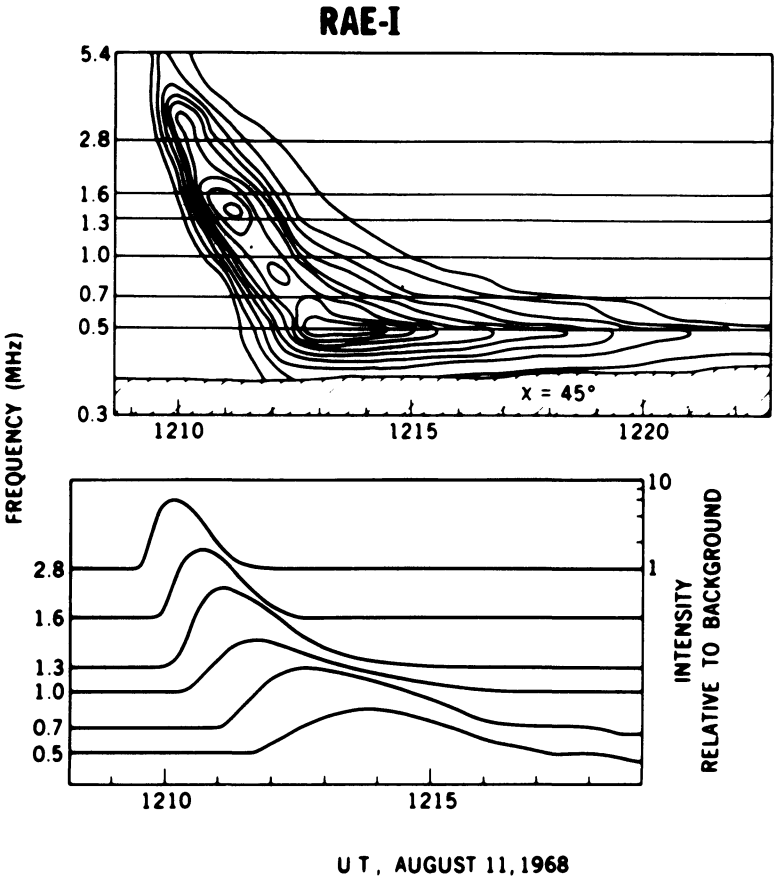

Fig. 1. Dynamic spectrum of a type III burst at hectometer wavelengths observed with the RAE-1 satellite. The upper figure shows a computer-developed dynamic spectrum from 5.4 to 0.3 MHz with 1-dB intensity contours. The lower figure shows the intensity profiles at six frequencies corresponding to the horizontal lines through the upper figure.

The properties of such bursts can be described in terms of certain measurable burst parameters:

(a) Onset time – the time at which the burst rises to a detectable amount above background. This time indicates the arrival of the fastest particles in the exciter at the appropriate coronal level.

(b) Peak time – the time of burst maximum. This time indicates the arrival of the more numerous average-energy particles in the exciter at the corresponding coronal level.

(c) Decay time – Single bursts in the low-frequency region always have an exponential decay. For large bursts, this phase may extend for 5 decades of intensity and indicates a damping process with a rate of energy loss proportional to the amount of energy remaining. The decay time is usually defined as the *e*-folding time during the exponential decay. This quantity has been interpreted as the decay of plasma waves due to electron-ion collisions. There are several problems with this. Temperatures derived from observed decay times at very low frequencies are an order of magnitude lower than expected. Alvarez and Haddock (1973) have suggested that an additional electron-ion collisional energy exchange introduced by Wolff *et al.* (1971) to explain electron-proton temperatures at 1 AU will also account for the radio decay rates. Zaitsev *et al.* (1972) have suggested that Landau damping of plasma waves by the tail of the exciter will affect the decay rate and they have calculated burst profiles from a one-dimensional analysis. Although the predicted burst shapes seem to agree well with observations of small bursts this is not the case for large bursts where the theoretical profiles have decays much more rapid than the observed exponental decays. In addition, Harvey and Aubier (1973) have recently shown that in the solar wind where the plasma waves are convected into regions of decreasing density, the waves should experience a sudden abrupt attenuation due to Landau damping in the medium, but this is also not observed. It may be that some burst plasma waves can escape this fate by propagating towards the Sun to compensate for the outward solar wind convection. An additional interesting result which may not have physical significance is that the number of oscillation cycles within the decay time remains remarkably constant over the full range of type III observations.

(d) Excitation time – the time from the burst onset to when the decay first becomes uniformly exponential. The excitation time is taken (Aubier and Boischot, 1972) to be the effective duration of the burst exciter at a particular plasma level. The increase in excitation time at lower frequencies can be interpreted in terms of the growth in exciter length due to the dispersion of velocities in the exciter.

(e) Drift rate (onset or peak) – frequency drift rate between closely-spaced frequencies. This important quantity depends on the separation between the two emission levels, the velocity of the exciter, and the path difference to the observer. Drift times have been used often to derive information about emission levels.

(f) Cutoff frequencies. The dynamic spectra of most bursts have a high- and low-frequency limit. In satellite observations there is a tendency for the upper frequencies to be cut off for western events and for the low frequencies to be cut off for eastern events.

Other burst parameters which can be determined are burst intensity, burst size and burst arrival direction.

3. Storms of Type III Bursts

Although large type III events are well associated with flares, the great proportion of observable type III's are associated with storm periods (Fainberg and Stone, 1970a)

lasting for intervals of several days to over one solar rotation period. Figure 2 shows one such storm period in August 1968 about 4 days before central meridian passage (CMP) of the active region. Note the steady succession of drifting events and their drift rates. In Figure 3 the same storm is shown near CMP. Note the more rapid drift rates in this case. This is due to the fact that the low frequencies have a shorter

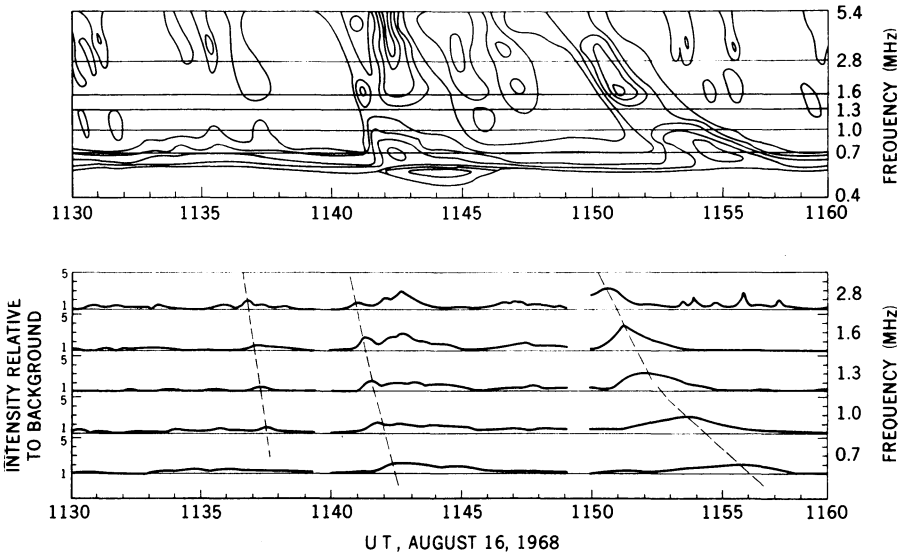

Fig. 2. A 30-min segment of data of a solar storm of type III bursts 4 days prior to CMP. The drift in frequency, limited burst bandwidth, and large numbers of small bursts can be seen.

radiation travel path than the higher frequencies – a time of flight effect discussed by Wild *et al.* (1959). The increased activity is probably due to refractive focusing of electromagnetic waves in the radial direction. The occurrence rate of one burst per 10 s suggests that several hundred thousand storm bursts may be released during one solar rotation.

In addition to bursts there is also a continuum component to the storms (Fainberg and Stone, 1971a). Figure 4 shows this for the August 1968 storm. The points plotted are the minimum background values for each 10-min interval during this period and represent the levels between bursts. These storm periods are also well associated with decametric storms and with metric type I storms (Sakurai, 1971; Stewart and Labrum, 1972).

I would like to close my discussion of storms by showing the variation of drift rates during the storm in Figure 5. Here, for each day of a 14-day period, the number distribution of observed drift times as a function of drift time is plotted. It is clear that a systematic variation of drift times occurs which depends on the orientation of the active region with respect to central meridian. By utilizing a three-parameter drift-time function depending on exciter speed, level separation, and CMP time, a least-

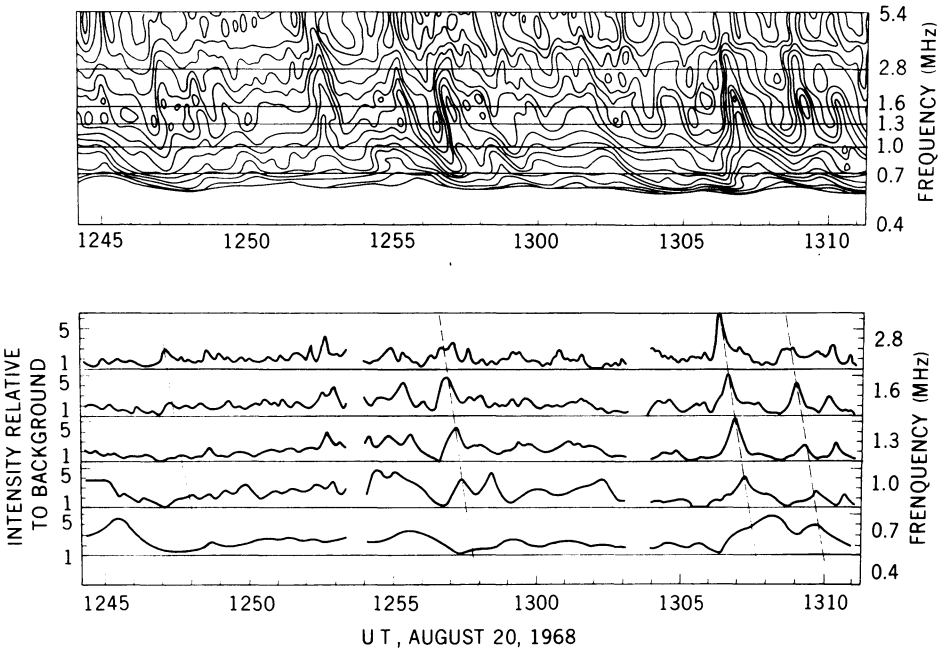

Fig. 3. A 30-min segment of data from the same storm as Figure 2, but near CMP. The higher occurrence rate and faster drift rate of the bursts are evident.

squares fitting procedure was followed to derive best fits of these quantities simultaneously from 2500 bursts. The scale so derived is presented in Figure 6. In this figure the bottom line represents the best estimate of coronal densities near solar minimum made by Newkirk (1967). The region between 10 $R_\odot$ and 215 $R_\odot$ is essentially an interpolation between values determined by light scattering and values from *in situ* measurements.

The radio data are plotted assuming that the observed radio frequency is at the plasma frequency. Reasons for believing that this assumption is questionable will be presented later. Slysh's (1967) point measured at 1 MHz results from a spin modulation plus lunar occultation measurement on several bursts observed by Luna 11 and 12. This technique determined the burst arrival direction from the spin modulation minima. The dashed line results from an extensive drift analysis of bursts observed by Hartz (1969) on the Alouette satellites. In this analysis, Hartz assumed an exciter speed of 0.35c and derived a set of level separations from the observed burst drift times. He also found his scale to be consistent with a pressure balance argument applicable to streamers using temperatures derived from burst decay rates. A similar analysis was made with other bursts observed on the ATS satellite by Alexander *et al.* (1969). The RAE points result from a drift-rate analysis of Fainberg and Stone (1970b, 1971b) in which exciter speed was also derived.

All of these analyses of type III emission levels, when converted to densities, indicate that the emission regions are enhanced in density by a factor of about 10. Close

https://doi.org/10.1017/S0074180900234232 Published online by Cambridge University Press

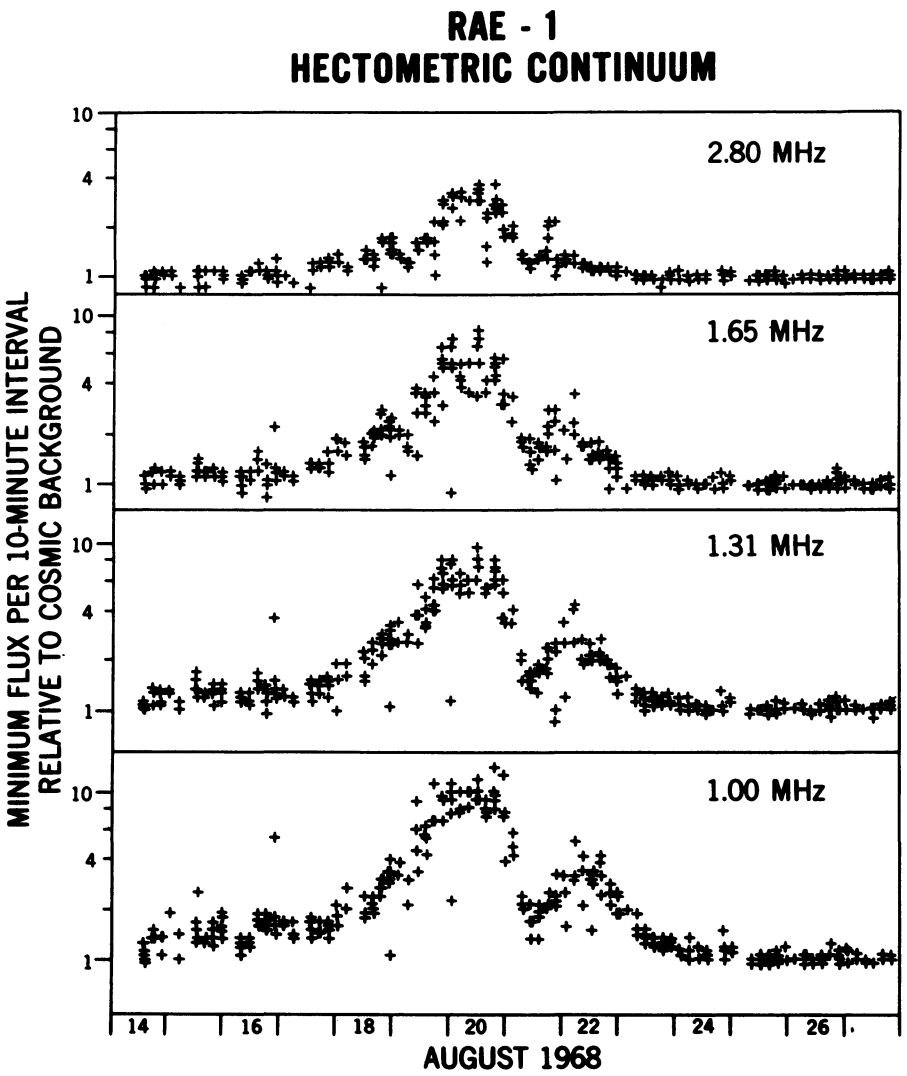

Fig. 4. The minimum flux values for 10-min periods of the August, 1968 storm as a function of heliographic longitude (day number) of the associated active region. The temporary decrease in storm activity on August 21 was also observed at metric frequencies. The minimum flux at the higher frequencies is essentially the level between bursts and represents the continuum component.

to the Sun, such enhancements are fairly common and could explain why type III emission can propagate to the Earth from limb events. However, optical measurements of density at increasing distances from the Sun do not support the assumption that enhancements occur often enough to account for the frequent occurrence of type IIIs.

With the launching of the IMP-6 satellite in 1971 the first results measured over a range of closely-spaced frequencies became available from a quiet spacecraft located

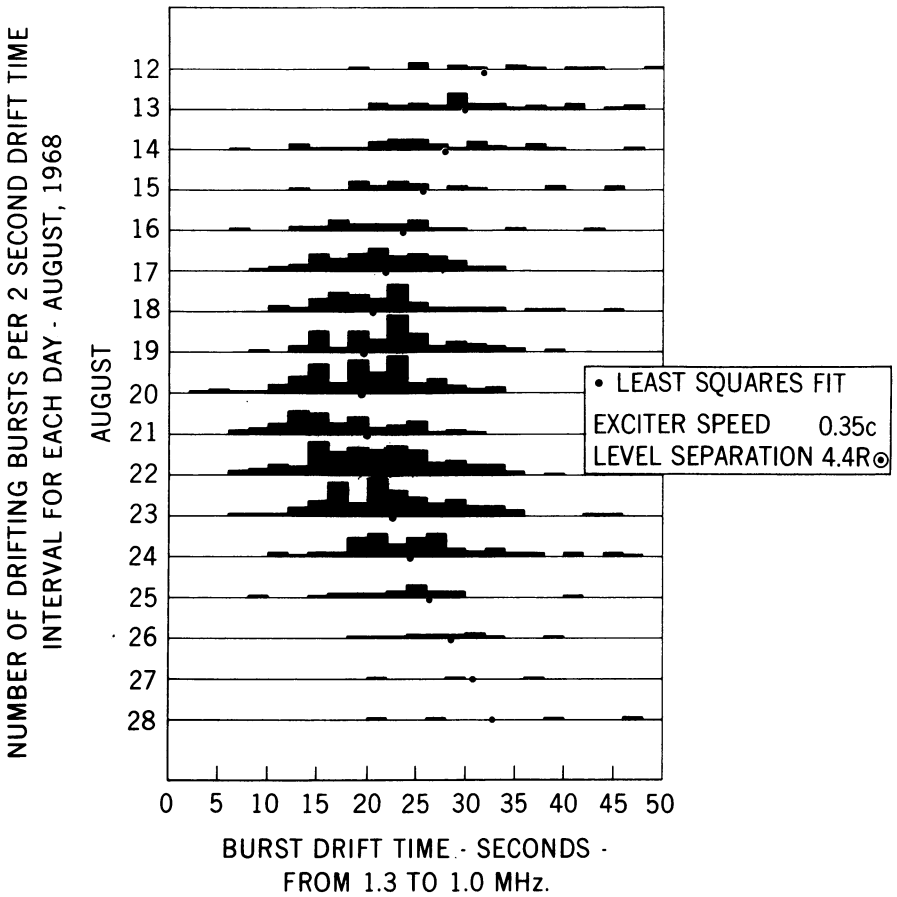

Fig. 5. The dependence of burst drift rate between 1.3 and 1.0 MHz on heliographic longitude for the August, 1968 storm. The least-squares fit, indicated by black circles in the figure, gives a level separation of 4.4 $R_\odot$ and an average exciter speed of 0.35 c.

well out in the solar wind. Figure 7 (Fainberg *et al.*, 1972) illustrates a typical single event going down to low frequencies. Here we have plotted the intensity-time profiles of the burst envelopes observed at a number of frequencies by the GSFC experiment on IMP-6. Note that the vertical scale is logarithmic; this burst is over 40 dB above background at mid-frequencies. This large western event had a high-frequency cutoff near 1 MHz and was not observed by ground equipment at Clark Lake Radio Observatory in the decameter range.

The insert in this figure illustrates the observed modulation pattern caused by the rotation of the dipole antenna in the spin plane (which is the same as the ecliptic plane). The minima of this pattern occur when the dipole axis passes closest to the source direction; the maxima occur 90 deg later when the antenna is broadside to the source direction. From an accurate knowledge of antenna orientation from optical sensors, we can determine the direction of arrival of the radiation with respect to the Sun–Earth

https://doi.org/10.1017/S0074180900234232 Published online by Cambridge University Press

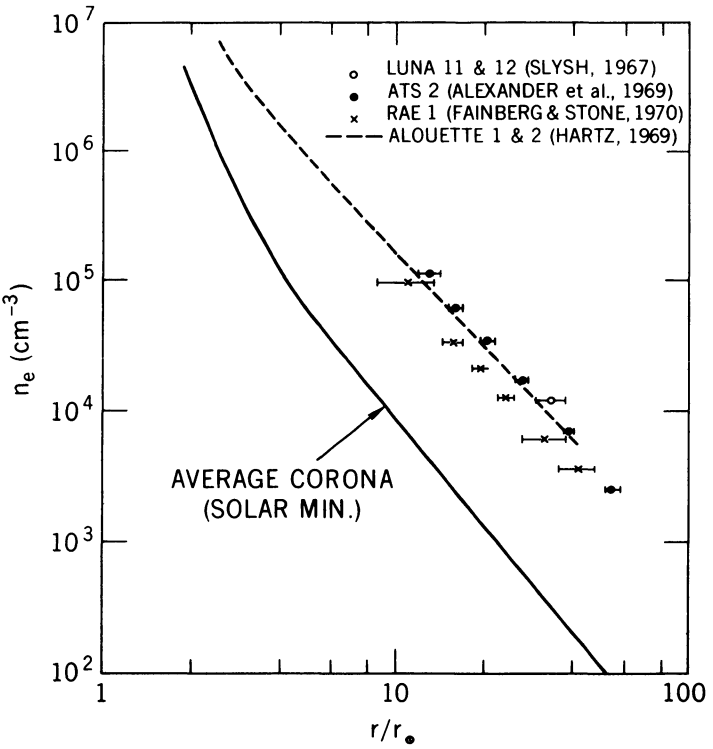

Fig. 6. Electron density vs distance from the Sun in the outer corona. The solid curve represents the values given by Newkirk (1967) as best estimates during solar minimum. The values given by the radio measurements are from single bursts and are placed assuming the type III radiation was observed at the fundamental of the local plasma frequency. They should be displaced downward a factor of 4 if the radiation was observed at twice the plasma frequency.

line. We have developed a very powerful data-processing technique which utilizes the entire waveform to derive the radio arrival direction. An error analysis indicates that with several minutes of data we can determine burst arrival directions to within 1 deg for small sources. It is clear that from a study of limb events the radio limb of the Sun can be determined at a wide range of frequencies. To interpret these results fully, it will be necessary to include effects of scattering and refraction discussed by Steinberg (1972).

In addition to burst arrival direction, we can also measure the depth of modulation accurately. This quantity, M, which we call the modulation index we define as

$$M = \frac{I_{\max} - I_{\min}}{I_{\max} + I_{\min}},$$

where $I_{\max}$ and $I_{\min}$ are the maximum and minimum intensities observed during one spin period. M has values between 0 and 1. A fully modulated burst with modulation index of 1 occurs only when a point source is located in the spin plane so that the antenna nulls pass through the source. A modulation index less than one results from a

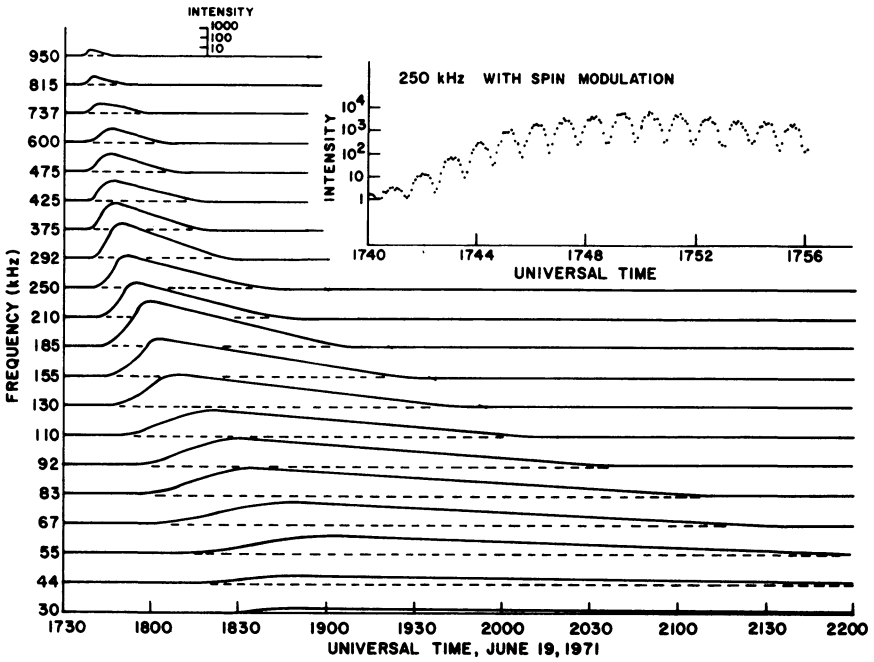

Fig. 7. A type III burst observed between 1 MHz and 30 kHz by the IMP-6 radio experiment. The insert figure illustrates the observed spin modulation at a frequency of 250 kHz, while for the main figure, only the burst envelopes are shown for clarity.

distributed source centered in the spin plane or from a smaller source located out of the plane. Within this range of ambiguity, which we have explored, we can determine some information on source size.

Figure 8 shows the results of this data-processing technique applied to the burst of Figure 7. The positions of the Earth and Sun are shown in the ecliptic plane. From spin modulation we determined the source direction to be along the lines labeled by the frequency of observation. The open circles on this figure are the distances of closest approach to the Sun which form a lower bound on emission levels for the burst. An extrapolation of the emission level scale derived in RAE storm analysis yields intersections of the emission lines with the emission surfaces represented by the solid circles. In examining many limb events, we have found that this scale is a reasonable one to use. It is understood that further refinements in such a scale will occur when the effects of scattering and refraction (Steinberg, 1972) are taken into account.

For this burst we have found that the modulation index becomes essentially zero at 55 kHz, implying that the radiation was nondirective and arrived isotropically to the antennas, so that this emission originated close to 1 AU. Note the spiral configuration of the burst trajectory resulting from the interplanetary magnetic field.

Figure 9 shows these results plotted on a density scale. The lower line is an interpolation between light-scattering results at 10 $R_\odot$ and long term *in situ* measurements at 1 AU. The upper line is the RAE scale. The open circles are the minimum emission

https://doi.org/10.1017/S0074180900234232 Published online by Cambridge University Press

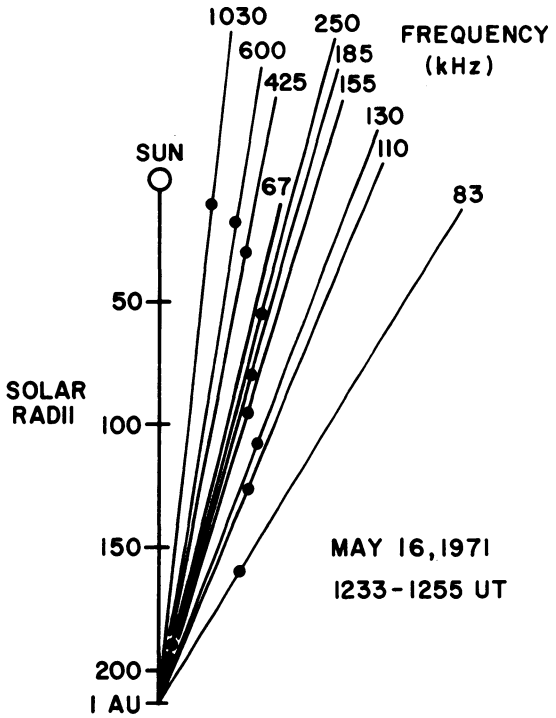

Fig. 8. Directions of arrival (in the ecliptic plane) determined from the spin modulation for the burst in Figure 7. The trajectory shown by the black dots is fixed by using the RAE-1 emission level scale (see text). The trajectory shown by the open circles is determined by the distance of closest approach permitted by the arrival direction.

levels permitted by the distance of closest approach. Again, we see a density enhancement by an order of magnitude, even out to 1 AU. Direct measurements of such enhancements are very rare and this strongly motivates one to seek other interpretations. The most obvious one is that the low-frequency bursts are observed at the harmonic of the plasma frequency, which then drops the radio density levels on this diagram by a factor of 4. In many thousands of type III bursts observed by RAE and IMP-6 with good frequency resolution from 5 MHz down, we have never seen a convincing fundamental-harmonic pair of type III bursts and this suggests that we are looking primarily at one class or the other. The densities derived from the emission levels favor the harmonic interpretation.

Recently Haddock and Alvarez (1973) have interpreted many low-frequency complex type III events observed on OGO-5 as having fundamental and harmonic components. They find there is a transition frequency below several MHz where the observed burst changes from predominantly fundamental radiation at higher frequencies to predominantly harmonic radiation at lower frequencies. However, multicomponent complex events can be deconvolved in different ways; in the absence of published profiles it is not clear how uniquely the data support this interesting conclusion.

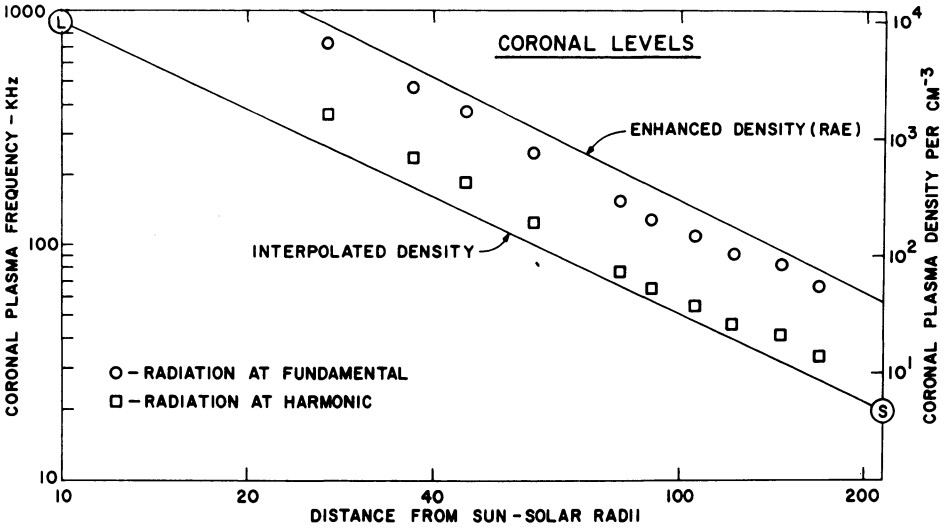

Fig. 9. Interplanetary density and plasma frequency scale as a function of distance in solar radii. The interpolated density scale is given by a line between the value determined by light-scattering observations, labeled *L*, and that from space probe measurements, labeled *S*. The circles are the density scale corresponding to the closest approach trajectory shown in Figure 8, assuming radiation occurs at the plasma frequency. These points map into the squares if radiation occurs at the second harmonic of the plasma frequency.

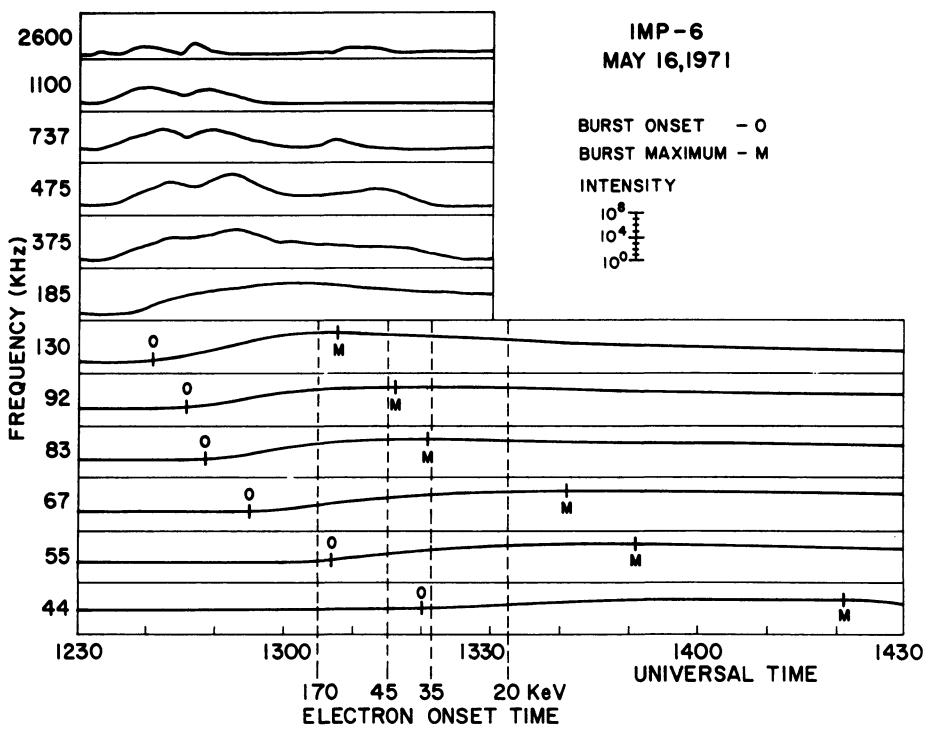

Fig. 10. Intensity-time profiles (spin modulation removed) of a type III burst observed on 16 May 1971 for frequencies from 2600 kHz to 44 kHz. The loss of spin modulation at 55 kHz places this level at 1 AU. Note the observed electron onset times.

https://doi.org/10.1017/S0074180900234232 Published online by Cambridge University Press

Additional evidence for the harmonic interpretation at low frequencies comes from IMP-6 observations of type II radiation which is clearly observed at both the fundamental and harmonic frequencies (Malitson *et al.*, 1973a). An analysis of one event reported by Malitson *et al.* (1973b) strongly indicates that the position of the type II fundamental agrees with the RAE type III scale only if the III's are observed at the harmonic of the plasma frequency. In addition to these arguments there is the association of radio burst onset time with energetic electrons reported by Lin *et al.* (1973). Figure 10 shows the comparison for one event in May, 1971. For this event, the loss of modulation at 55 kHz indicates that this level was near 1 AU. The series of electron onset times measured by Lin shows that the radio burst onset agrees with the onset of 170-keV electrons. As the arrival of the more numerous slower electrons occurs, the radio burst increases in intensity with the burst maximum corresponding to the onset of approximately 10-keV electrons. These data strongly suggest that the beam energy conversion causing the radio burst takes place at the leading edge of the electron stream where velocity separation of electrons in transit causes a positive slope on the differential energy spectrum (Zaitsev *et al.*, 1972; Lin *et al.*, 1973). Figure 11 shows the trajectory of this radio burst. Again, the dots are the intersections of the measured arrival directions with emission-level surfaces determined from the RAE scale. We see that this is again a western event with the burst trajectories out-

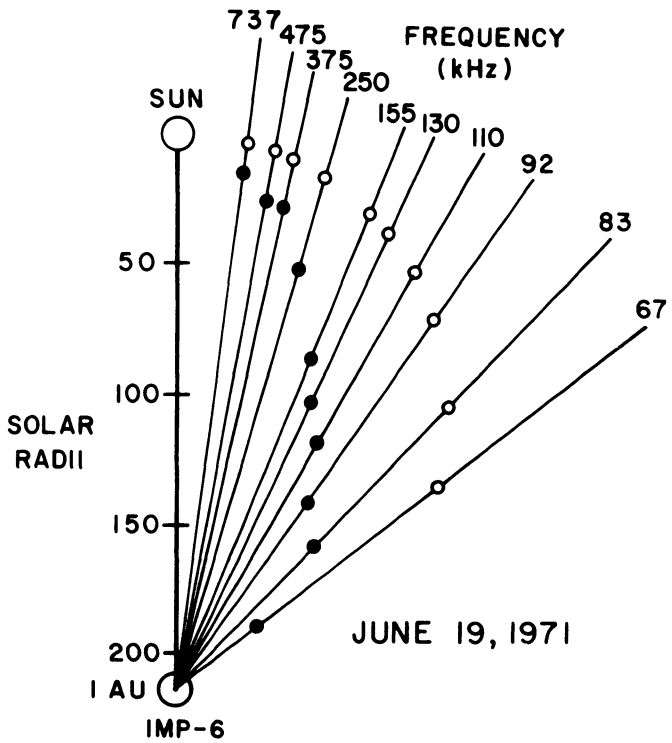

Fig. 11. Average trajectory of the type III burst for which simultaneous electron measurements were made. See Figure 10.

https://doi.org/10.1017/S0074180900234232 Published online by Cambridge University Press

lining the spiral curvature of the magnetic field. This figure is a summary over the history of the burst. In order to look for dynamic changes we have developed techniques for computer processing the IMP-6 data to generate movies of solar bursts in progress.

Figure 12 shows the format of the plots. The plane of the figure is the ecliptic with

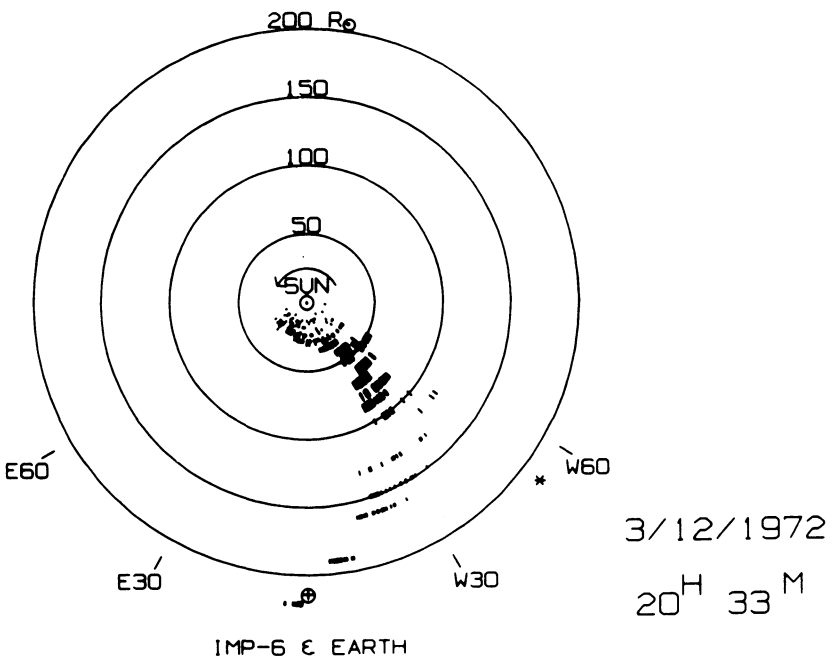

Fig. 12. Format of a computer-generated plot of data from IMP-6. The plane of the figure is the ecliptic with IMP-6 and Earth located at bottom – ⊕. For each minute of data, the intersection of the measured type III arrival directions with the spherical emission level is determined, and a radial line segment with length proportional to log intensity is plotted. This figure is a collection of data from 32 frequencies taken at 5-s intervals for a 2-min period.

west to the right and east to the left. A grid of four concentric circles separated by 50 $R_\odot$ is plotted. A fifth innermost circle is at 5 $R_\odot$, just under the arrow showing the direction of solar rotation; we note how these satellite observations complement ground-based observations by pointing out that ground-based measurements deal with phenomena occurring within the 5 $R_\odot$ circle.

For each minute of spin-modulated data we determine the arrival direction. We then calculate the intersection of this direction with the spherical emission level given by the RAE scale and plot a radial line segment whose length is proportional to the logarithm of the burst intensity above background. Each frame of the movie is a collection of these intersections for a certain period of the burst – usually for 5 min. Successive movie frames differ by 5 s so that there is a steady progression in time. In this single frame we see a solar burst in the process of moving out from the Sun.

Figure 13 shows a sequence of frames separated by 2 min taken from this movie.

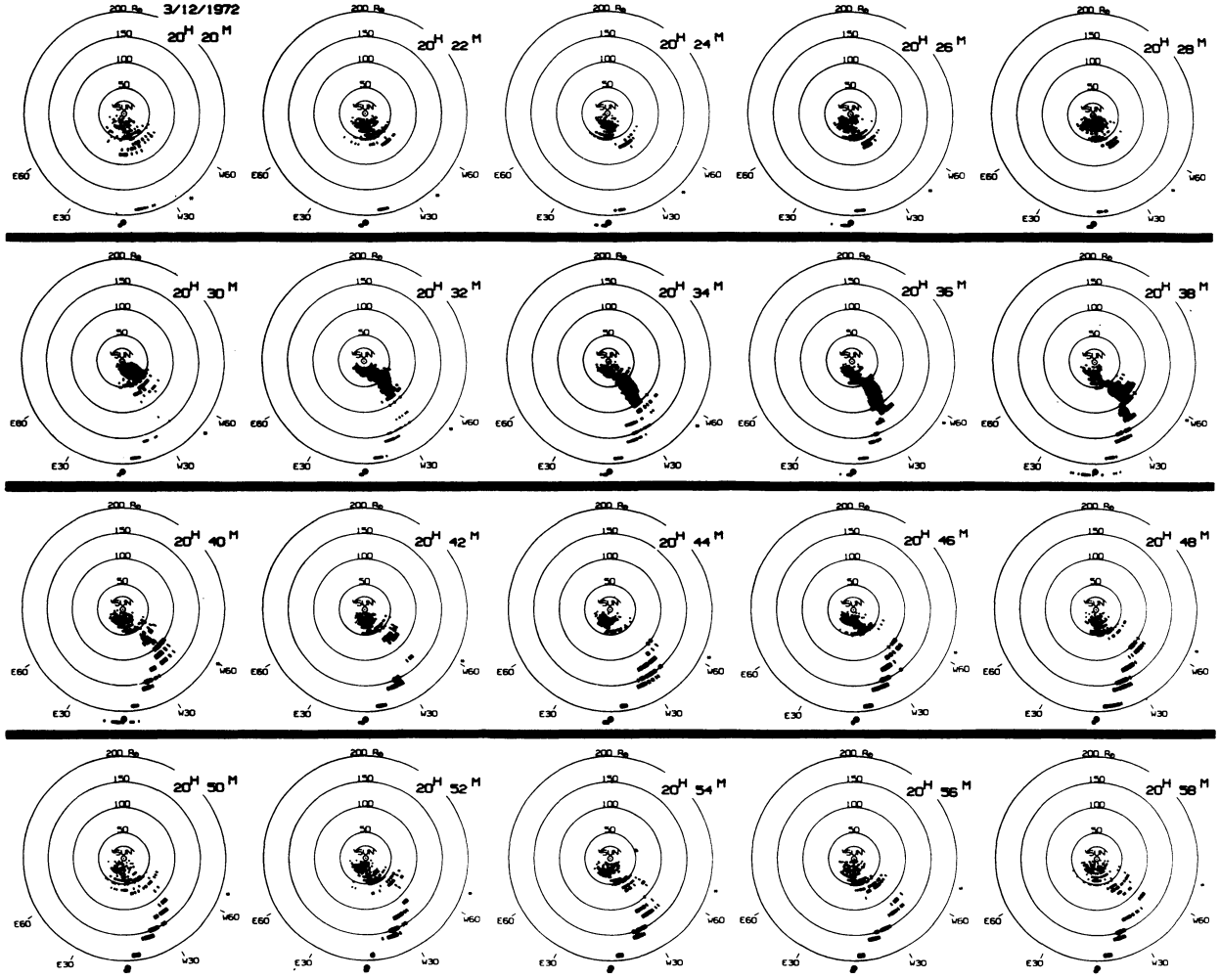

Fig. 13. Frames separated by 2-min intervals during a large type III burst. A low-level solar storm visible over the first $\frac{1}{3}$ AU is present before and after the burst.

Fig. 14. Two type III bursts showing a low-frequency cutoff. The bursts are not visible beyond 40 $R_\odot$.

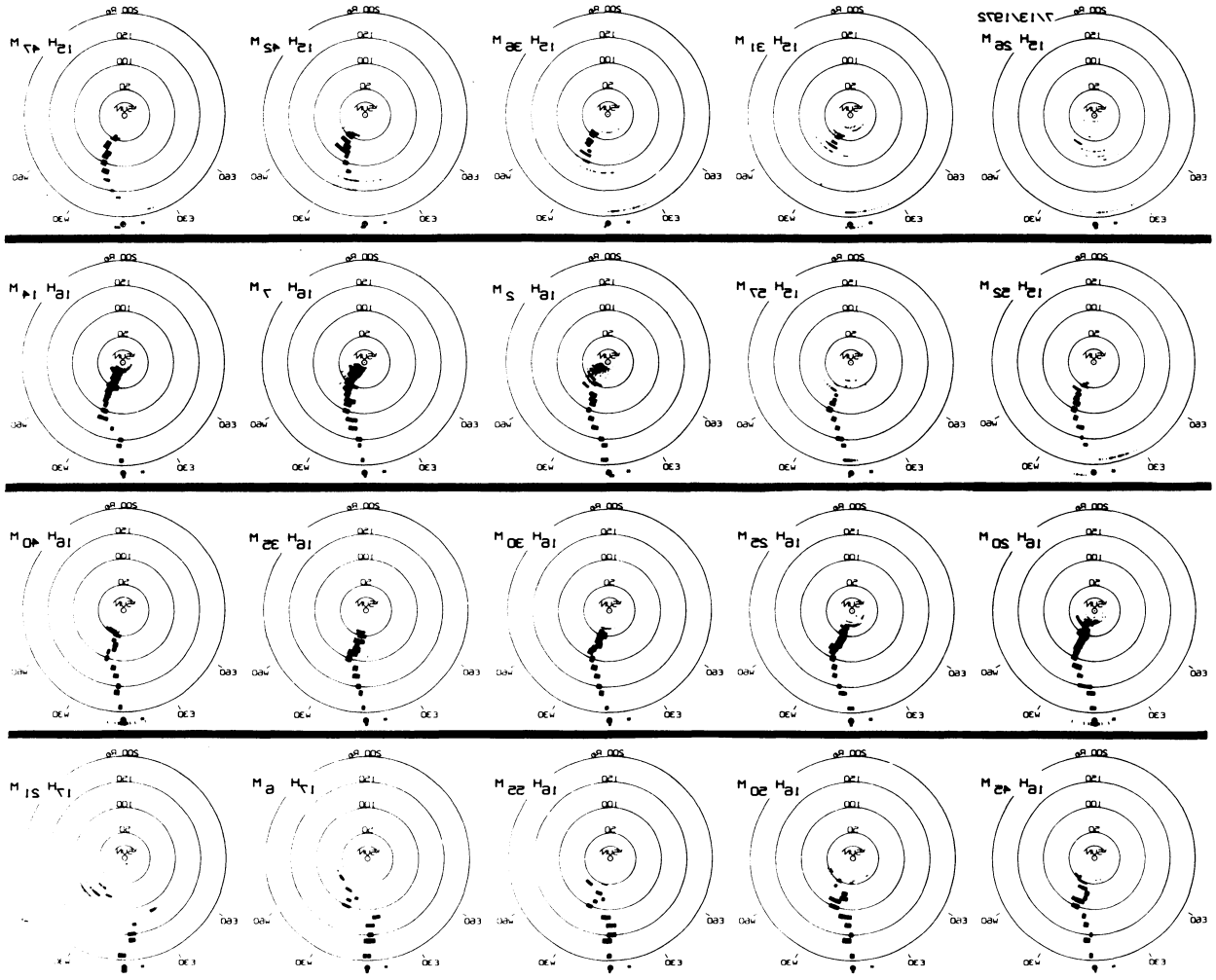

Fig. 15. Two type III bursts. The first, starting near 1531 UT, shows no high-frequency components although it is quite large. The second burst, starting near 1602 UT, does have high-frequency components.

Prior to the burst there is a long-lasting solar storm in progress, consisting of many overlapping small bursts visible out to 70 $R_\odot$. At 2026 UT, a type III becomes visible near the Sun and the emission region progresses outward as the exciter electrons propagate along the interplanetary magnetic field. At 2036 UT, the main part of the exciter is at 50–100 $R_\odot$ while the fastest particles have already reached 1 AU. The spiral structure of the interplanetary magnetic field is outlined by this burst.

Very often, type III bursts have a limited frequency range over which they are visible. Figure 14 shows a sequence of frames from 2 bursts on 12 July 1972 which are normal type III events, but without low-frequency components. Such bursts are fairly common, especially during storms. They may indicate interplanetary magnetic field conditions which cause the burst exciter packet to become very diffuse as it moves out.

Figure 15 shows an example of a type III burst without high-frequency components. This burst first becomes visible near 45 $R_\odot$ at 1531 UT and moves out to 1 AU. At 1602 UT, a second type III burst starts much closer to the Sun and progresses outward along a similar trajectory. It may be that the first burst is an example of electron acceleration by magnetic field reconnection at large distances from the Sun. It is clear that a wide range of interplanetary phenomena can be explored by these radio techniques.

There is very great interest in out-of-the-ecliptic configurations. The second RAE spacecraft was launched in July of this year into lunar orbit. For the first several weeks it was in a spinning mode with just the dipoles extended. We placed the axis of spin in the ecliptic plane and perpendicular to the Sun–Earth line so that we could determine arrival directions out of the ecliptic. We should get additional information from lunar occultation. The only solar burst we have examined is consistent with a trajectory out from the Sun inclined about 10° to the ecliptic. The next spinning spacecraft will be Helios A which will go in to about $\frac{1}{4}$ AU from the Sun and will be launched in 1974.

Goddard also has a joint experiment with Steinberg's group at Meudon on the IME spacecraft, set for 1978. This will involve the synthesis of a spinning tilted dipole so that the two angles defining the arrival direction can be determined; in addition, source size can be found. This will allow the tracking of solar bursts out of the ecliptic and will yield the radio determination of magnetic field configurations extending outside the ecliptic plane.

The ideal situation would be to have two spinning spacecraft simultaneously measuring the same burst from an extended baseline. This would permit triangulation to determine source location and would allow a direct determination to be made of emission levels as well as source directivity. With fewer space launches being planned, it is not clear when such an opportunity might occur.

References

Alexander, J. K., Malitson, H. H., and Stone, R. G.: 1969, *Solar Phys.* **8**, 388.

Alvarez, H. and Haddock, F. T.: 1973, in R. Ramaty and R. G. Stone (eds.), *High Energy Phenomena on the Sun*, NASA SP-342, Washington.

Aubier, M. and Boischot, A.: 1972, *Astron. Astrophys.* **19**, 343.
Fainberg, J. and Stone, R. G.: 1970a, *Solar Phys.* **15**, 222.
Fainberg, J. and Stone, R. G.: 1970b, *Solar Phys.* **15**, 433.
Fainberg, J. and Stone, R. G.: 1971a, *Astrophys. J.* **164**, L123.
Fainberg, J. and Stone, R. G.: 1971b, *Solar Phys.* **17**, 392.
Fainberg, J., Evans, L. G., and Stone, R. G.: 1972, *Science* **178**, 743.
Haddock, F. T. and Alvarez, H.: 1973, *Solar Phys.* **29**, 183.
Hartz, T. R.: 1969, *Planetary Space Sci.* **17**, 267.
Harvey, C. C. and Aubier, M. G.: 1973, *Astron. Astrophys.* **22**, 1.
Lin, R. P., Evans, L. G., and Fainberg, J.: 1973, *Astrophys. Letters* **14**, 191.
Malitson, H. H., Fainberg, J., and Stone, R. G.: 1973a, *Astrophys. Letters* **14**, 111.
Malitson, H. H., Fainberg, J., and Stone, R. G.: 1973b, *Astrophys. J.* **183**, L35.
Newkirk, G., Jr.: 1967, *Ann. Rev. Astron. Astrophys.* **5**, 213.
Sakurai, K.: 1971, *Solar Phys.* **16**, 125.
Slysh, V. I.: 1967, *Kosm. Issled.* **5**, 897; *Cosm. Res.* **5**, 759.
Steinberg, J. L.: 1972, *Astron. Astrophys.* **18**, 382.
Stewart, R. T. and Labrum, N. R.: 1972, *Solar Phys.* **27**, 192.
Weber, R. R., Alexander, J. K., and Stone, R. G.: 1971, *Radio Sci.* **6**, 1085.
Wild, J. P., Sheridan, K. V., and Neylan, A. A.: 1959, *Australian J. Phys.* **12**, 369.
Wolff, C. L., Brandt, J. C., and Southwick, R. G.: 1971, *Astrophys. J.* **165**, 18.
Zaitsev, V. V., Mityakov, N. A., and Rapoport, V. O.: 1972, *Solar Phys.* **24**, 444.